

## Generated Flow in Fluid Medium by Focused Ultrasound: Acoustic Streaming PIV Measurements

Rafika Ben Haj Slama<sup>1,\*</sup>, Bruno Gilles<sup>2</sup>, Maher Ben Chiekh<sup>1</sup>, Jean-Christophe Béra<sup>2</sup>

<sup>1</sup>Laboratory of thermal and energy systems studies, ENIM, University of Monastir, Monastir, Tunisia

<sup>2</sup>Laboratory of Therapeutic Applications of Ultrasound, INSERM U1032, University of Lyon1, Lyon, France

\*rafika.ben-haj-slama@inserm.fr

---

**Abstract** The use of ultrasound for therapeutic and diagnostic applications has become common and it has been shown that High Intensity Focused Ultrasound (HIFU) could be a new therapeutic tool to relieve several cardiovascular diseases. For this reason, it is imperative to investigate different hydrodynamic and acoustic aspects related to focused ultrasound. In this context, an experimental study of acoustic streaming, was performed. In order to determine velocity field driven during ultrasound application, Particle Imaging Velocimetry (PIV) technique was used. Tests were conducted using a focused transducer that emits at a 500 kHz frequency, and which was immersed in a degassed and filtered water tank. Water was seeded with spherical Polyamide Seeding Particles. For PIV analyses and post processing, an open-source tool (PIVlab in MATLAB) [1] was used for image cross-correlation and velocity field resolution. Otherwise, these tests were performed with a parametric variation, namely, the imposed acoustic pressure (varying from 2.3 to 7.4 bars) and the seeding particles size (ranged from 5 to 50  $\mu\text{m}$  diameter with a respective concentration of 0.09 to 0.18  $\text{g}/\text{m}^3$ ). Experimental results allowed us to conclude that: (i) Ultrasound radiation force acting on the seeding particles can influence their behavior: According to the tests performed, 5 $\mu\text{m}$ -diameter seeding particles seem to be the most reliable and the most appropriate to characterize the flow, while 20 and 50 $\mu\text{m}$ -diameter particles are dispersed and removed from the ultrasound focal zone to the shearing zone due to interactions with the acoustic field. (ii) For ultrasound-subjected flow, streaming axial velocity is of the order of millimeters per second, and this streaming velocity is increasing with ultrasonic amplitude. As expected, the velocity field has the shape of the ultrasonic intensity field in the focal area, with a downstream shift of the maximal velocity position compared to the focal position.

**Keywords:** Focused ultrasound, acoustic streaming, velocity field, particle image velocimetry, seeding particles

---

### 1 Introduction

Nowadays, cardiovascular diseases have become the leading cause of death worldwide and their treatments are complicated and risky. For example, a thrombus in artery or in vein, which is simply a severe blood vessel obstruction, requires invasive pharmacological and surgical treatments such as coronary bypass or angioplasty. Extracorporeal High-Intensity Focused Ultrasound seems to be a potentially interesting way to ensure a non-invasive treatment of thrombolysis [2][3][4][5][6] and may be a cure for this type of cardiovascular diseases. It has been shown that the principal mechanism involved in sonothrombolysis is cavitation, which destroys clots effectively. Acoustic streaming is, also, another phenomenon that contributes significantly to the effectiveness of sonothrombolysis. This phenomenon can improve the mixing in the treatment area, and thus increase the efficiency of thrombolytic agents. However, the major problem with this alternative is the risk of releasing clot fragments in blood circulation causing downstream obstruction of smaller vessels [6].

Several questions arise, then, about how effective thrombolysis is, about its optimization and about the risk it may presents. That being so, it is imperative to study several hydrodynamic and acoustic aspects related to focused ultrasound, and it is in this context we performed an experimental study of acoustic streaming phenomenon which is flow caused by acoustic energy absorption during wave propagation in the medium. At high frequencies (over 500 kHz), a non-zero averaged velocity appears in the liquid due to viscous dissipation of acoustic energy per volume. This nonlinear phenomenon is called Eckart streaming [7]. The acoustic streaming phenomenon has been known since the 1830s [8][9] and has been the subject of numerous fundamental publications. However, few studies compare the theoretical, numerical and experimental results, especially, for focused ultrasound. Therefore, it is essential to establish an experimental database highlighting this hydrodynamic aspect, to validate numerical models and to identify their limitations. Experimental measurements of the acoustic streaming, with PIV technique, were already

conducted [10][11][12][13]. And several seeding particles were used; namely hollow glass beads of 10µm diameter size, spherical polyamide particles of 50µm diameter size and pine pollen powder. In the literature, authors do not mention their seeding particles selection criteria nor the optimal concentration of these particles; that allow them to ensure a good PIV quality.

In this study, acoustic streaming was investigated with seeding particles of different sizes, and we have shown that for acoustic streaming PIV-measurement, large seeding particles can be influenced by acoustic forces so that streaming flow will not be reliably tracked. Furthermore, Computational Fluid Dynamics (CFD) study, which reproduces the same experimental setup, was also proposed. This numerical approach was compared with the experimental approach.

## 2 Governing equations

For an incompressible and Newtonian fluid, and if we take into account steady state of the streaming flow in the presence of acoustic stress, the acoustic streaming motion can be defined by the following equations [14] [15]:

$$“\vec{u} \nabla u = -\frac{1}{\rho_0} \nabla p + \nu \nabla^2 \vec{u} + \vec{F}” \quad (1)$$

$$“F_i = -\frac{\partial(\overline{\rho u_i u_j})}{\partial x_i},” \quad (2)$$

Where  $F$ , is the volume force associated with the Reynolds stress given by  $\overline{(\rho u_i u_j)}$ ,  $\rho_0$  is the density of the propagation medium,  $u$  is the streaming velocity,  $p$  is the acoustic pressure and  $\nu$  is the kinematic viscosity. For an incompressible fluid, mass conservation law is:

$$“\rho_0 \frac{\partial \bar{u}_i}{\partial x_i} = 0” \quad (3)$$

For focused and axisymmetric spherical transducer, the governing equations for the streaming field in infinite medium read:

$$“\frac{\partial \bar{u}_x}{\partial x} + \frac{1}{r} \frac{\partial(r \bar{u}_r)}{\partial r} = 0” \quad (4)$$

$$“\bar{u}_r \frac{\partial \bar{u}_x}{\partial r} + \bar{u}_x \frac{\partial \bar{u}_r}{\partial x} = \frac{F_x}{\rho_0} - \frac{1}{\rho_0} \frac{\partial \bar{p}}{\partial x} + \nu \left[ \frac{\partial^2 \bar{u}_x}{\partial x^2} + \frac{1}{r} \frac{\partial}{\partial r} \left( r \frac{\partial \bar{u}_x}{\partial r} \right) \right]” \quad (5)$$

$$“\bar{u}_r \frac{\partial \bar{u}_r}{\partial r} + \bar{u}_x \frac{\partial \bar{u}_r}{\partial x} = -\frac{1}{\rho_0} \frac{\partial \bar{p}}{\partial r} + \nu \left[ \frac{\partial^2 \bar{u}_r}{\partial x^2} + \frac{1}{r} \frac{\partial}{\partial r} \left( r \frac{\partial \bar{u}_r}{\partial r} \right) \right]” \quad (6)$$

Where  $x$  is propagation axis component and  $r$  is the radial distance from the ultrasonic beam axis.

## 3 Experimental procedure and methods

### 3.1 Experimental set up

To generate the ultrasonic waves, a spherically focused transducer (with a 10 cm diameter, and a 10 cm focal length), was set up. Piezoelectric transducer resonance frequency was at 550 kHz. The driving signal of the transducer comes from a generator (Model: Tektronix AFG 3102, 100 MHz) which supplies an input voltage, respectively, of 50, 100 and 150 mV in continuous mode, generating an acoustic pressure amplitude at the focus, respectively, of 2.3, 5.5 and 7.4 bars.

Ultrasound tests were conducted in 60l-tank of degassed and filtered water (rate of dissolved gas in water < 2mg/l). The water was seeded with spherical polyamide particles PSP (Polyamid Seeding Particles, Dantec Dynamics) whose density, which is very close to that of water, is of 1030 kg.m<sup>3</sup> [16]. It is, generally, convenient to introduce a quantity of particles with such a concentration that interrogation window

comprises 5 to 20 particles [17][18]. The present work, tests were conducted with three different seeding particles sizes (diameter of 5, 20 and 50 microns), whose concentration was, for all tests, between 10 and 20 particles per interrogation area which corresponds to a concentration varying from 0.09 to 0.18 g/m<sup>3</sup>.

The used laser source was an MGL-F-532-2W with a wavelength of 532 nm, operating in continuous and pulsed mode, depending on the test carried out, and generates a 2mm-diameter light beam. In order to enlarge the beam, an optical system consisting of a lens assembly, has been designed and implemented. This allowed us to obtain a 20cm wide and 1mm thickness laser sheet, which is enough to highlight the acoustic streaming phenomenon.

A CMOS-based high-speed camera (Phantom V12.1 Vision Research) has been used to record streaming flow, and to process acquired images. In terms of visualization parameters, the resolution was of 1280 x 800 pixels, the frame rate was of 24 frames per second and the exposure time was of 41 ms, with a field of view of 9cm x 5.6cm. Figure 1 shows our experimental setup.

Acoustic streaming measurement was initiated with the positioning of acoustic propagation axis within the laser plane. Following this, the ultrasound was turned on and the flow field near the focus was allowed to reach steady state in 60s before recording.

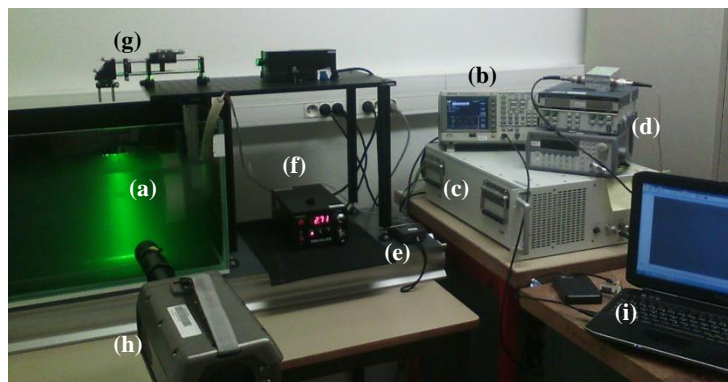


Fig. 1 Experimental configuration: {Acoustic streaming generation system: (a) Ultrasound transducer immersed in a 60l water tank, (b) Voltage generator, (c) Amplifier, (d) wattmeter, (e) thermocouple}, {PIV measurement system: (f) Laser generator, (g) Optical assembly, (h) CMOS camera, (i) Data acquisition}

### 3.2 Velocity field resolution

To solve the streaming velocity field, acquired images were processed. Images cross-correlation was performed using PIVlab, which is a set of routines built in MATLAB [1], and adopting Fast Fourier Transform algorithm (FFT). This algorithm is iterative and based on an initial assessment of velocity vectors on large interrogation area (128 pixels x 128 pixels in our study), corresponding to a high signal-to-noise ratio (SNR) due to the large number of particles in the interrogation area. This initial velocity field was then used in the following iterations or passes, where interrogation area is gradually reduced to, finally, reaches a size of 32x32 pixels or 16x16 pixels, that depends on cases.

It should be noted that preprocessing was applied to raw images before starting the velocity field resolution in order to improve contrast, reduce noise, and homogenize the intensities of image particles, and thereafter avoid polarization of the cross-correlation function for the larger particles (diameter=50 $\mu$ m).

Regarding post-treatment of correlated frames and for data validation, local median filter or normalized median test, proposed by Westerveel and Sacarano [19], was chosen. This filter was applied for the focal zone where there is a local streaming flow. As for the far-streaming field where velocity is almost zero, we set a vector velocity threshold with a very low standard deviation compared to the average velocity.

### 4 Results:

In this section we present the effect of focused ultrasound on particle flow nature, and we will highlight the streaming driven by the absorption of high amplitude acoustic oscillations. PIV tests were conducted with varying seeding particles size and gradually increasing the applied acoustic pressure (the generator voltage to the input). The obtained results are summarized in Figure 2. This figure shows the axial velocity component in the plane (x, y); where x is the propagation direction of the ultrasonic wave and y is the radial component.

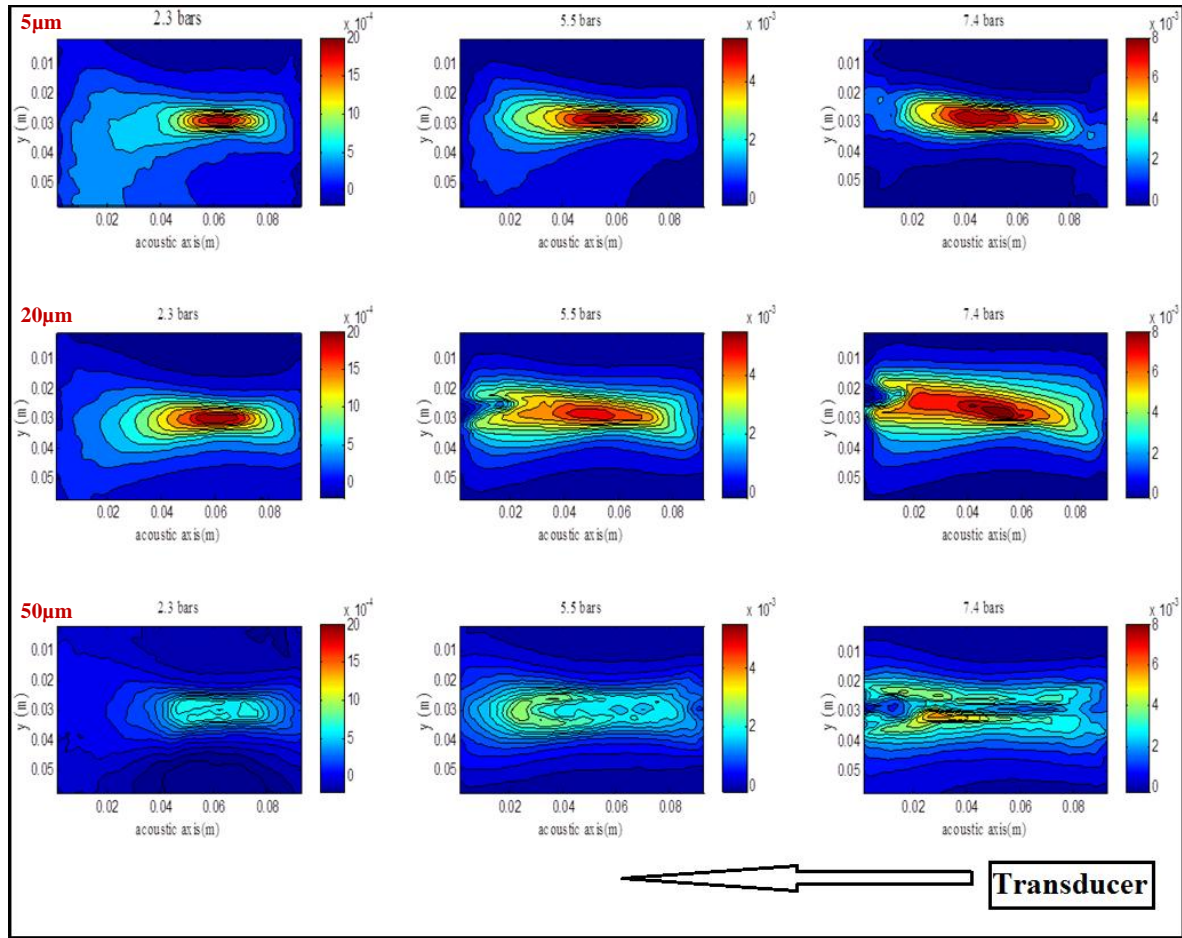


Fig. 2 Axial particle velocity field (m/s) in the laser plane (x, y), Top: Particle Diameter=5µm, middle: Particle Diameter=20µm, Bottom: Particle Diameter=50µm. Geometric focus abscises=0.062m

According to figure 2, we can notice that PIV-measured velocity fields are similar, in terms of maximum amplitude, for small and mid-range particles. While, for large particles, velocity values are much lower in the ultrasonic focal zone. And when increasing the acoustic pressure, a stopping point upstream of the transducer geometric focus is observed. We can see, more clearly, the different behavior of the large particles in the acquired images (see Figure 3). Indeed, when acoustic intensity increases, large particles do not penetrate any more in high pressure focal zone upstream of the transducer focus, and over time the particles cluster grow more and more, and a breakpoint forms.

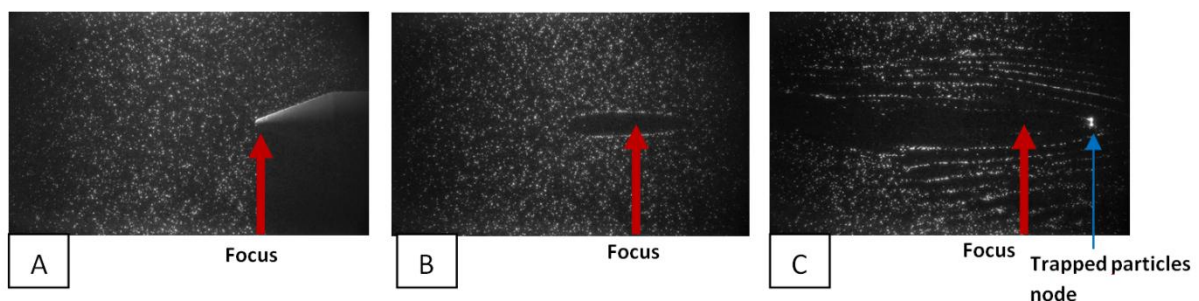


Fig. 3 Particles distributions. A: without ultrasound, B: medium subjected to low acoustic intensity (corresponding to V<sub>e</sub>=50mV), C: medium subjected to high acoustic intensity (corresponding to V<sub>e</sub>=250mV)

To investigate whether the flow nature changes in the presence of large particles and to see what exactly is going on in the focal zone, a test was made by seeding with both; small particles (assumed to perfectly

follow the flow) and large particles. An illustration of this test is given in Figure 4.

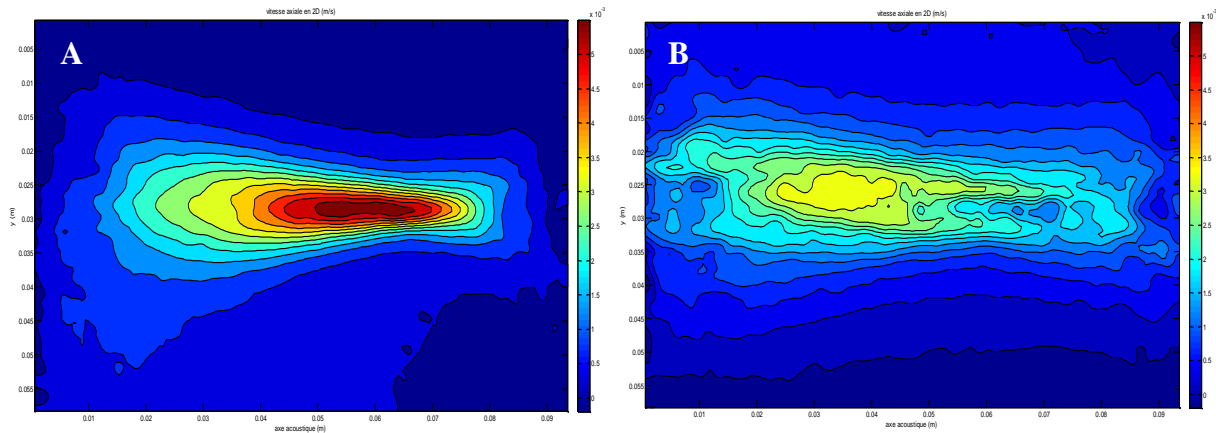


Fig.4 PIV Particle velocity field in the same acoustic field (5.5 bars). A: 5 $\mu$ m-diameter particles only, B: 5 and 50 $\mu$ m-diameter particles.

Based on these results we can conclude that large particles undergo acoustic forces, and no longer follow the flow. Consequently, they are no longer suitable for PIV in the presence of acoustic forces. For this reason we will be limited to tests with small particles to characterize the streaming field during ultrasound application. Figures 5 and 6 show velocity evolution on the acoustic axis depending on the applied acoustic intensity, for small and mid-range particles. These figures show that for low applied intensities ( $V_e = 50$  mV,  $P_{ac} = 2.3$  bar) velocity peak position on acoustic axis coincides with the geometric focus. And as the intensity increases ( $V_e > 100$  mV) the peak position is increasingly shifted from focus.

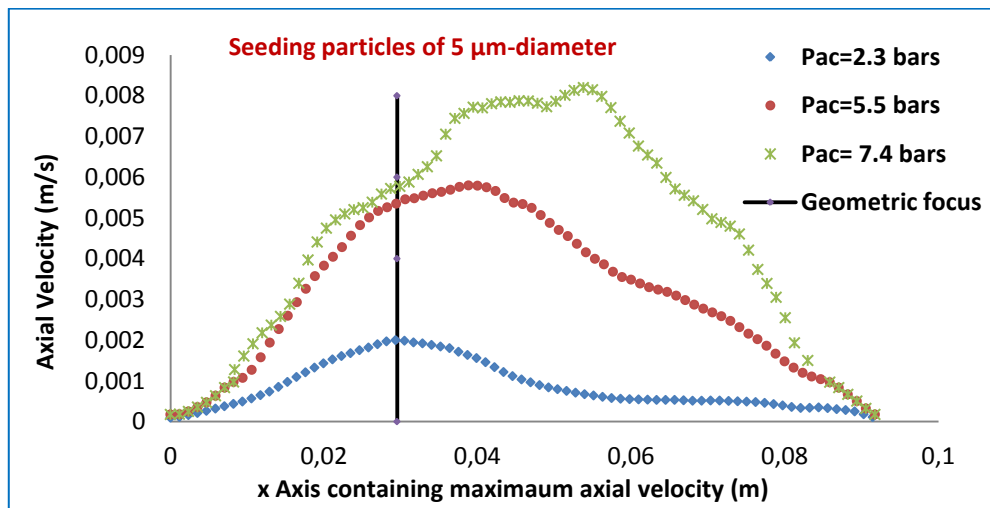


Fig.5 Axial particle velocity profile comparison depending on inlet acoustic pressure. Case of 5 $\mu$ m-diameter seeding particles

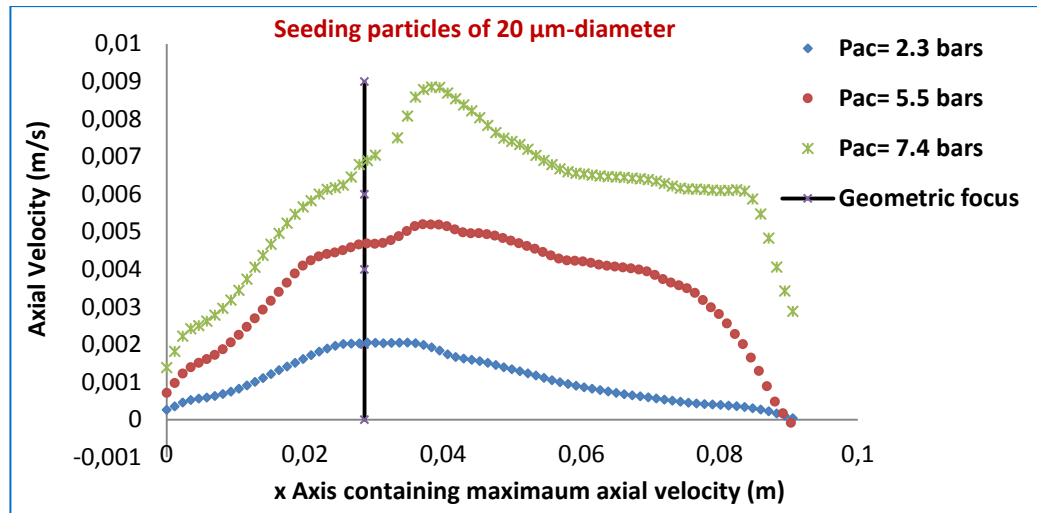


Fig.6 Axial Particle velocity profile comparison depending on inlet acoustic pressure. Case of 20µm-diameter seeding particles

The following table summarizes the maximum velocity values reached, depending on applied acoustic intensities.

Table. 1 Maximum axial velocity reached in focal zone (m/s)

|          | Ve=50 mV<br>≡<br>Pac=2.3bars | Ve=100 mV<br>≡<br>Pac=5.5bars | Ve=150 mV<br>≡<br>Pac=7.4bars |
|----------|------------------------------|-------------------------------|-------------------------------|
| Ø=5 µm   | 2 X 10 <sup>-3</sup>         | 5.8 X 10 <sup>-3</sup>        | 8.2 X 10 <sup>-3</sup>        |
| Ø =20 µm | 2 X 10 <sup>-3</sup>         | 5.2 X 10 <sup>-3</sup>        | 8.6 X 10 <sup>-3</sup>        |
| Ø =50 µm | 0.6 X 10 <sup>-3</sup>       | 2 X 10 <sup>-3</sup>          | 3 X 10 <sup>-3</sup>          |

From the comparison of velocity profiles on the acoustic axis (see figures 5 and 6), we observe that the “Gaussian shape” is larger for mid-range particles which means that they are longer driven beyond the focal zone relatively to the small particles. This is another reason to use only small particles to characterize the acoustic streaming field.

Numerical simulations with Fluent © were conducted to confirm the streaming field measured by 5µm-particles and we have reproduced the experimental case to validate the numerical approach and ensure the reliability of implemented model. Simulation results are summarized in Figure 7. It is a comparison of streaming velocity amplitude. For the numerical simulations, velocity throughout the acoustic axis is illustrated, as to the experiments, it is the velocity along the axis passing through the maximum amplitude (the experimental velocity fields are not symmetric).

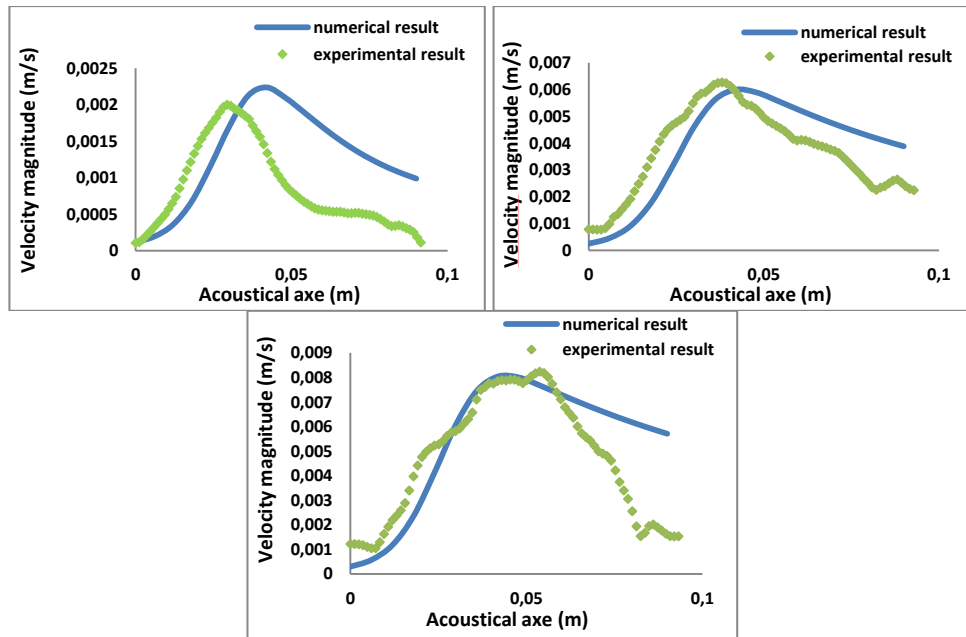


Fig. 7 PIV Streaming velocity and CFD streaming velocity comparison, left: Acoustic pressure=2.3 bar, right: Acoustic pressure=5.5bar, bottom: Acoustic pressure=7.4bar

Except for the case where acoustic pressure is low (50mV), the maximum velocity amplitude obtained by the simulation is similar to that obtained by the experimental tests. The Gaussian profile is almost confused upstream of the focus and presents a significant gap downstream from focus. This could be explained by experimental positioning imprecision and by the fact that the medium is considered infinite in the simulations when actually it is not the case.

## 5 Discussion

In recorded movies it was found that the large particles are dispersed from the focal zone and that they are faced to an obstacle made of particle cluster upstream of the geometric focus (see Figure 3). This leads us to think that this behavior is due to an acoustical effect and these particles are not reliable and suitable for PIV in the presence of ultrasound. To confirm it, a jet flow in absence of ultrasound and whose velocity field is known in advance, has been solved by PIV and seeded with large particles. A syringes pump was used to set a rate of 10 ml/min and a jet velocity of 2.2 cm/s. This test was performed to see if the larger particles behave in the same way in jet zone as in the presence of focused ultrasound. The result is given in Figure 9.

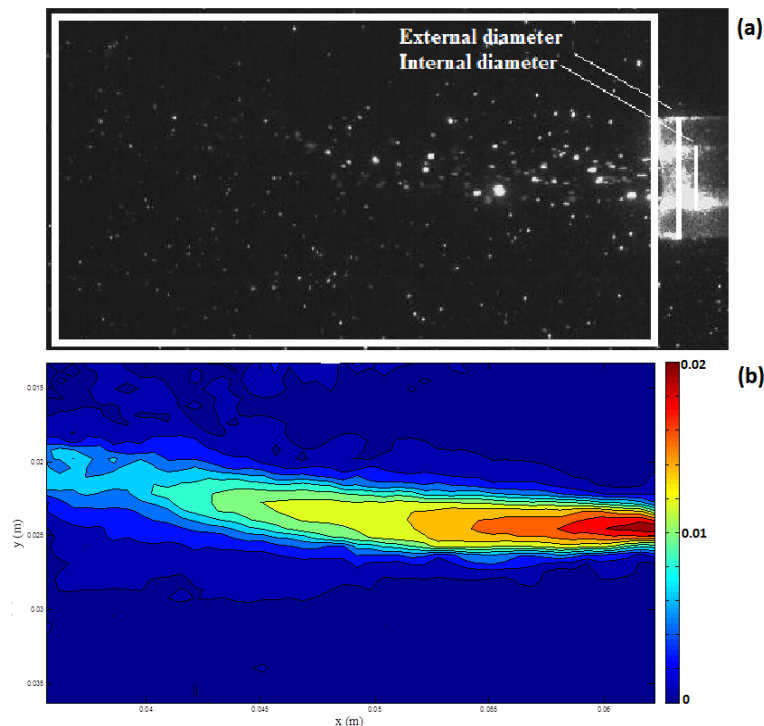


Fig. 8 PIV validation test with a known jet flow. (a): Acquired image, (b): Axial velocity field (m/s) obtained by PIV

According to Figure 8 (a), the particles are not dispersed from the jet zone, unlike the case of acoustic streaming jet. And from Figure 8 (b), outlet tube velocity obtained by PIV is 0.02 m/s, thus showing an error of only 9% compared to the estimated real velocity. So we can say that phenomenon that happens in figure 3 is entirely acoustical and the large particles undergo acoustic forces so they are no longer reliable to describe the flow in the presence of ultrasound.

## 6 Conclusions

In this study, we are interested in therapeutic ultrasound thrombolysis, especially the fluid dynamic behavior during treatment in focal zone. Acoustic streaming was studied by PIV technique and modeled using Fluent solver. The main result of this study is that: Ultrasound radiation force acting on the seeding particles can influence particle behavior: According to the tests performed, only 5 $\mu$ m-diameter seeding particles seem to be reliable and appropriate to characterize the flow, while 20 and 50 $\mu$ m-diameter particles, usually suitable for PIV-measurement of equivalent hydrodynamic flows, are disqualified for measurement of ultrasound-streaming flows. This point has not been taken into account in previous study related to acoustic streaming PIV investigations. Results allowed us also to show that, as expected, the velocity field corresponding to ultrasound-subjected flow, has the shape of the ultrasonic intensity field in the focal area. Streaming axial velocity is of the order of several millimeters per second and is increasing with ultrasonic amplitude, specifically varying from 2 to 8 millimeters per second with imposed acoustic pressure respectively varying from 2.3 to 7.4 bars. Numerical and experimental Gaussian profiles are almost confused upstream of the focal zone and present a significant gap downstream from focus. This can be explained by the fact that fluid field is considered infinite in CFD tests when actually it is not the case. In this way and in future works we plan to conduct experimental and numerical investigations related to bounded or confined field configurations (cylindrical tube, contracted vessel ...).

## Acknowledgments

This work is supported in one hand by the Rhône-Alpes Region (Project CMIRA 2015, and in the other hand, by the LabEx CelyA (Project : ANR-10-LABX-0060). Both are gratefully acknowledged.

## References



- [1] Thielicke W and Stamhuis E J (2014) PIVlab – Time-Resolved Digital Particle Image Velocimetry Tool for MATLAB (version 1.4).
- [2] Siegel R J, Luo H (2008) Ultrasound Thrombolysis. *Ultrasonics*, vol.48(4), pp 312-20.
- [3] Hong A S, Chae J S, Dubin S B, Lee S, Fishbein M C, Siegel RJ (1990) Ultrasonic Clot Disruption: An in Vitro Study. *American Heart Journal*, vol. 120(2), pp 418-22.
- [4] Luo H, Nishioka T, Fishbein M C, Cercek B, Forrester J S, Kim C J (1996) Transcutaneous Ultrasound Augments Lysis of Arterial Thrombi in Vivo. *Circulation*, vol. 94(4), pp775-8.
- [4] Rosenschein U, Furman V, Kerner E, Fabian I, Bernheim J, Eshel Y (2000) Ultrasound Imaging-Guided Noninvasive Ultrasound Thrombolysis: Preclinical Results. *Circulation*, vol.102(2), pp 238-45
- [6] Maxwell A D, Cain C A, Duryea A P, Yuan L, Gurm H S, Xu Z (2009). Noninvasive Thrombolysis Pulsed Ultrasound Cavitation Therapy-Histotripsy. *Ultrasound in Medicine and Biology*, vol.35(12), pp1982-94.
- [7] Eckart C (1948) Vortices and Streams Caused by Sound Waves, *Phys. Rev*, vol. 73, pp 68-76.
- [8] Faraday M (1831), Acoustic Streaming, *Phil. Trans.*, vol.121, pp 229.
- [9] Rayleigh L (1929) The Theory of Sound , *MacMillan, London*.
- [10] Nowicki A , Kowalewski T, Secomski W, Wojccik J (1998) Estimation of Acoustical Streaming: Theoretical Model, Doppler Measurements and Optical Visualization, *European Journal of Ultrasound*, vol.7, pp 73-81.
- [11] Hariharan P, Myers M R, Robinson R A, Maruvada S H, Silwa J, Banerjee R K (2008) *Journal of Acoustic Society of America*, pp 1706-1719.
- [12] Luo Tan A C H and Hover F S (2009) Correlating the Ultrasound Thrust Force with Acoustic Streaming Velocity, *Institute of Electrical and Electronics Engineering IEEE International*, pp 2627-2630.
- [13] Moudjed B, Botton V, Henry D, Ben Hadid H and Garandet J P (2014) Scaling and Dimensional Analysis of Acoustic Streaming Jet, *Physics of Fluids*, vol.26, 093602.
- [14] Lighthill J (1978) Acoustic Streaming, *Journal of Sound and Vibration*, vol. 61, pp 391-418.
- [15] Lighthill J (1978) *Waves in Fluids*, Cambridge University Press, Cambridge,U.K.
- [16] DANTEC Dynamics, SAFEX® Fog Generator Systems, “Safe seeding for Flow visualisation and LDA applications”
- [17] Keane R D and Adrian R J (1992) Theory of Cross-correlation Analysis of PIV Images, *Applied Scientific Research*, vol.49, pp 191–215.
- [18] Thielicke W and Stamhuis E J (2014) PIVlab – Towards User-friendly, Affordable and Accurate Digital Particle Image Velocimetry in MATLAB, *Journal of Open Research Software*, 2: e30
- [19] Westerweel J and Scarano F (2005) Universal Outlier Detection for PIV Data, *Experiments in Fluids*, vol.39, pp 1096–1100.